

# Strong longitudinal color-field effects in $pp$ collisions at energies available at the CERN Large Hadron Collider

V. Topor Pop,<sup>1</sup> M. Gyulassy,<sup>2</sup> J. Barrette,<sup>1</sup> C. Gale,<sup>1</sup> and A. Warburton<sup>1</sup><sup>1</sup>*McGill University, Montreal, Canada H3A 2T8*<sup>2</sup>*Columbia University, New York, New York 10027, USA*

(Received 4 November 2010; published 7 February 2011)

We study the effect of strong longitudinal color fields (SCF) in  $p + p$  reactions up to Large Hadron Collider (LHC) energies in the framework of the HIJING/ $\bar{B}\bar{B}$  (v2.0) model that combines (collinear factorized) perturbative quantum chromodynamics multiple minijet production with soft longitudinal string excitation and hadronization. The default vacuum string tension,  $\kappa_0 = 1$  GeV/fm, is replaced by an effective energy-dependent string tension,  $\kappa(s) = \kappa_0(s/s_0)^{0.06}$  that increases monotonically with center-of-mass energy. The exponent  $\lambda = 0.06$  is found sufficient to reproduce well the energy dependence of multiparticle observables in the Relativistic Heavy Ion Collider, Tevatron, as well as recent LHC data. This exponent is half of that predicted by the color glass saturation (CGC) model,  $\lambda_{\text{CGC}} = 0.115$ , where gluon fusion multiparticle production mechanisms are assumed. In HIJING/ $\bar{B}\bar{B}$  (v2.0), the rapid growth of  $dN_{\text{ch}}/d\eta$  with energy is due to the interplay of copious minijet production with increasing SCF contributions. The large (strange) baryon-to-meson ratios measured at Tevatron energies are well described. A significant enhancement of these ratios is predicted up to the highest LHC energy (14 TeV). The effect of  $J\bar{J}$  loops and SCF on baryon-antibaryon asymmetry, and its relation to baryon number transport, is also discussed.

DOI: [10.1103/PhysRevC.83.024902](https://doi.org/10.1103/PhysRevC.83.024902)

PACS number(s): 12.38.Mh, 24.85.+p, 25.40.Ve, 25.75.-q

## I. INTRODUCTION

With the commissioning of the Large Hadron Collider (LHC), it will soon be possible to test models of multiparticle production in hadron-hadron collisions up to an energy of 14 TeV. Charged particle densities,  $dN_{\text{ch}}/d\eta$ , especially the values at midrapidity and their dependence on center-of-mass energy  $\sqrt{s}$ , are important for understanding the mechanism of hadron production and the interplay of soft and hard scattering contributions in the LHC energy range. The rate of parton-parton and multiple parton-parton (MPI) scattering are strongly correlated to the observed particle multiplicity (related also to *initial entropy* and *initial energy density* generated in the collision process). New data on inclusive charged particle distributions from the LHC in  $pp$  collisions have become available [1–12]. These results complement previous data on  $pp$  and  $p\bar{p}$  collisions taken at lower energies  $\sqrt{s} = 0.02$ –1.96 TeV [13–23]. Many of these measurements have been used to constrain phenomenological models of soft-hadronic interactions and to predict properties at higher energies [24–37]. The recent LHC data may lead to a better theoretical understanding based on a quantum chromodynamics (QCD) approach [38–41].

The heavy ion jet interacting generator (HIJING) [42] and HIJING/ $\bar{B}\bar{B}$  (v1.10) models [43] have been used extensively to study particle production in  $pp$  collisions and to determine the physical properties of the ultradense matter produced in relativistic heavy-ion collisions. In the LUND [44] and dual-parton (DPM) [45] models multiple QCD strings or flux tubes were proposed to describe soft multiparticle production in longitudinal color fields. Color exchange between high  $x$  partons in the projectile and target create confined color flux tubes of tension ( $\approx 1$  GeV/fm) that must neutralize through pair production or color singlet hadronization approximately

uniformly in rapidity. In nucleus-nucleus collisions, the  $A^{1/3}$  enhancement of the local parton density of high  $x$  partons allows for higher color Casimir representations to be excited. Those flux tubes with stronger longitudinal color fields than in average  $pp$  reactions have been called color ropes [46] and naturally have higher string tensions [47]. Recently, an extension of color glass condensate (CGC) theory has proposed a more detailed dynamical “GLASMA” model [48,49] of color ropes.

In the HIJING model [42], the soft beam jet fragmentation is modeled by simple diquark-quark strings as in the LUND model with multiple gluon kinks induced by soft gluon radiations. Hard collisions are included with standard perturbative QCD (pQCD) as programed in the PYTHIA generator [50]. However, HIJING differs from PYTHIA by the inclusion of a geometric scaling multiple jet production model. Thus this model contains both longitudinal field-induced *soft* beam jet multiparticle production and collinear factorized pQCD based *hard* multiple jet production for  $p_T \geq p_0 = 2$  GeV/ $c$ .

A systematic comparison with data on  $pp$  and  $p\bar{p}$  collisions in a wide energy range [42] revealed that minijet production and fragmentation as implemented in the HIJING model provide a simultaneous and consistent explanation of several effects: the inclusive spectra at moderate transverse momentum ( $p_T$ ), the energy dependence of the central rapidity density, the two-particle correlation function, and the degree of violation of Koba-Nielsen-Olesen (KNO) scaling [51,52] up to Tevatron energy ( $\sqrt{s} = 1.8$  TeV). However, the model failed to describe the dependence of the mean value of transverse momentum ( $\langle p_T \rangle$ ) on charged-particle multiplicity ( $N_{\text{ch}}$ ). Wang argued [52] that by requiring high  $N_{\text{ch}}$  within a limited pseudorapidity ( $\eta$ ) range one necessarily biases the data toward

higher  $p_T$  minijets, hence the observed increase of  $\langle p_T \rangle$  versus (vs.)  $dN_{\text{ch}}/d\eta$  [52]. This effect has also been associated with the presence of transverse flow of the hadronic matter [53,54] and was proposed as possibly due to *quark-gluon plasma* (QGP) formation already in  $pp$  collisions.

Initial states of color gauge fields produced in high-energy heavy-ion collisions have also recently been discussed in Ref. [55]. Decay of a strong color electric field (SCF) ( $E > E_{\text{critical}} = 10^{18}$  V/m) due to the Schwinger mechanisms [56] plays an important role at the initial stage of heavy-ion collisions at ultrarelativistic energies. A thermalization scenario based on the analogy between Schwinger mechanisms and the Hawking-Unruh effect has been proposed [57]. It was also suggested that the back-reaction and screening effects of quark and antiquark pairs on external electric field could even lead to the phenomenon of plasma oscillations [58–60].

Recently, the Schwinger mechanism has been revisited [61] and pair production in time-dependent electric fields has been studied [62]. It was concluded that particles with large momentum were likely to have been created earlier, and for very short temporal widths ( $\Delta\tau \approx 10 t_c$ , where the Compton time  $t_c = 1/m_c$ ), and as a consequence the Schwinger formula could underestimate the reachable particle number density. In previous articles, we have shown that the dynamics of strangeness production in  $pp$  and Au + Au collisions at Relativistic Heavy Ion Collider (RHIC) energies deviates considerably from calculations based on Schwinger-like estimates for homogeneous and constant color fields and point to the contribution of fluctuations of transient SCFs [63–66].

In this article we extend our study of the dynamic consequences of SCF in the framework of the HIJING/B $\bar{B}$  (v2.0) model [64] to particle production in hadron-hadron collisions at LHC energies. We explore dynamical effects associated with long-range coherent fields (i.e, strong longitudinal color fields), including baryon junctions and loops [63,67], with emphasis on the new observables measured in  $pp$  collisions at the LHC by the ALICE, ATLAS, and CMS collaborations. Our study aims to investigate a broad set of observables sensitive to the dynamics of the collisions, covering both longitudinal and transverse degree of freedom. In addition, this study is intended to provide the  $pp$  baseline to future extrapolations to LHC studies of proton-nucleus ( $p + A$ ) and nucleus-nucleus ( $A + A$ ) collisions.

## II. OUTLINE OF HIJING/B $\bar{B}$ (v2.0) MODEL

In HIJING/B $\bar{B}$  (v2.0), in addition to conventional quark-diquark longitudinal electric fields, novel color flux topology junction antijunction ( $J\bar{J}$ ) loops are also implemented. In a dual superconductor model of color confinement for the three-quark positioning in a Y geometry, the flux tubes converge first toward the center of the triangle and there is also another component that runs in the opposite direction (like a Mercedes star) [68]. Unlike the conventional diquark-quark implemented in LUND and the HIJING model [42], the HIJING/B $\bar{B}$  (v1.10) [43] model allows the diquark-quark to split with the three independent flux lines tied together

with an  $\epsilon_{ijk}$  a junction and terminating on three delocalized fundamental Casimir quarks. We introduced [67] a new version (v2.0) of HIJING/B $\bar{B}$  that differs from HIJING/B $\bar{B}$  (v1.10) [43] in its implementation of additional more complex flux topologies via junction-antijunction ( $J\bar{J}$ ) loops. We parametrize the probability that a junction loop occurs in the string. Moreover, we enhance the intrinsic (anti-)diquark-quark  $p_T$  kick (by a factor  $f = 3$ ) of all ( $q$ - $qq$ ) strings that contain one or multiple  $J\bar{J}$  loops. The reason for this is the mechanism behind the dynamic of diquark-quark breaking (see Ref. [64] for details).

In string fragmentation phenomenology, it has been proposed that the observed strong enhancement of strange particle production in nuclear collisions could be naturally explained via SCF effects [47]. For a uniform chromoelectric flux tube with field ( $E$ ), the pair production rate [46,47,61] per unit volume for a heavy (light) quark ( $Q$ ) is given by

$$\Gamma = \frac{\kappa^2}{4\pi^3} \exp\left(-\frac{\pi m_Q^2}{\kappa}\right), \quad (1)$$

where  $Q = qq$  (diquark),  $s$  (strange),  $c$  (charm), or  $b$  (bottom). The *current quark masses* are  $m_{qq} = 0.45$  GeV [69],  $m_s = 0.12$  GeV,  $m_c = 1.27$  GeV, and  $m_b = 4.16$  GeV [70]. The *constituent quark masses* of light nonstrange quarks are  $M_{u,d} = 0.23$  GeV, of the strange quark is  $M_s = 0.35$  GeV [71], and of the diquark is  $M_{qq} = 0.55 \pm 0.05$  GeV [69].

Note that  $\kappa = |eE|_{\text{eff}} = \sqrt{C_2(A)/C_2(F)} \kappa_0$  is the effective string tension in low-energy  $pp$  reactions with  $\kappa_0 \approx 1$  GeV/fm and  $C_2(A)$ ,  $C_2(F)$  are the second-order Casimir operators (see Ref. [47]). An enhanced rate for spontaneous pair production is naturally associated with “strong chromoelectric fields” such that  $\kappa/m_Q^2 > 1$  *at least some of the time*. In a strong longitudinal color electric field, the heavier flavor suppression factor  $\gamma_{Q\bar{Q}}$  varies with string tension via the well-known Schwinger formula [56], since

$$\gamma_{Q\bar{Q}} = \frac{\Gamma_{Q\bar{Q}}}{\Gamma_{q\bar{q}}} = \exp\left[-\frac{\pi(M_Q^2 - m_q^2)}{\kappa_0}\right] < 1 \quad (2)$$

for  $Q = qq$ ,  $s$ ,  $c$ , or  $b$  and  $q = u$ ,  $d$ . In our calculations, we assume that  $M_{qq}^{\text{eff}} = 0.5$  GeV,  $M_s^{\text{eff}} = 0.28$  GeV,  $M_c^{\text{eff}} = 1.30$  GeV. Therefore, the above formula implies a suppression of heavier quark production according to  $u:d:qq:s:c \approx 1:1:0.02:0.3:10^{-11}$  for the vacuum string tension  $\kappa_0 = 1$  GeV/fm. For a color rope, on the other hand, if the *average string tension* value  $\kappa$  increases, the suppression factors  $\gamma_{Q\bar{Q}}$  increase. We show below that this dynamical mechanism improves considerably the description of the strange meson/hyperon data at the Tevatron and at LHC energies.

Saturation physics is based on the observation that small- $x$  hadronic and nuclear wave functions, and, thus the scattering cross sections as well, are described by the same internal momentum scale known as the *saturation scale* ( $Q_{\text{sat}}$ ). A recent analysis of  $pp$  data up to LHC 7 TeV has shown that, with the  $k_T$  factorized (GLR) gluon fusion approximation [72], the growth of the  $dN_{\text{ch}}/d\eta$  can be accounted for if the saturation

scale grows with center-of-mass energy as

$$Q_{\text{sat}}^2(s) = Q_0^2(s/s_0)^{\lambda_{\text{CGC}}}, \quad (3)$$

with  $\lambda_{\text{CGC}} \approx 0.115$ . The saturation scale is also increasing with atomic number as  $A^{1/6}$  [57]. It was argued that the effective string tension ( $\kappa$ ) of color ropes should scale with  $Q_{\text{sat}}^2$  [57,58].

However, in HIJING the string/rope fragmentation is the only soft source of multiparticle production and multiple minijets provide a semihard additional source that is computable within collinear factorized standard pQCD with initial and final radiation (DGLAP evolution [73]). In order to achieve a quantitative description, within our HIJING/B $\bar{B}$  framework we will show that combined effects of hard and soft sources of multiparticle production can reproduce the available data in the range  $0.02 < \sqrt{s} < 20$  TeV only with a reduced dependence of the effective string tension on  $\sqrt{s}$ . We find that the data can be well reproduced taking

$$\kappa(s) = \kappa_0 (s/s_0)^{0.06} \text{ GeV/fm} \approx Q_0 Q_{\text{sat}}(s), \quad (4)$$

where  $\kappa_0 = 1$  GeV/fm is the vacuum string tension value,  $s_0 = 1$  GeV<sup>2</sup> is a scale factor and  $Q_0$  is adjusted to give  $\kappa = 1.88$  GeV/fm at the RHIC energy  $\sqrt{s} = 0.2$  TeV. Our phenomenological  $\kappa(s)$  is compared to  $Q_{\text{sat}}^2(s)$  in Fig. 1, where  $\kappa = 1.40$  GeV/fm at  $\sqrt{s} = 0.017$  TeV increases to  $\kappa = 3.14$  GeV/fm at  $\sqrt{s} = 14$  TeV.

The energy dependence of the string tension leads to a variation of the diquark/quark suppression factors, as well as the enhanced intrinsic transverse momentum  $k_T$ . These include (i) the ratio of production rates of diquark-quark to quark pairs (diquark-quark suppression factor),  $\gamma_{qq} = P(qq\bar{q}\bar{q})/P(q\bar{q})$ ; (ii) the ratio of production rates of strange to nonstrange quark pairs (strangeness suppression factor),  $\gamma_s = P(s\bar{s})/P(q\bar{q})$ ; (iii) the extra suppression associated with a diquark containing

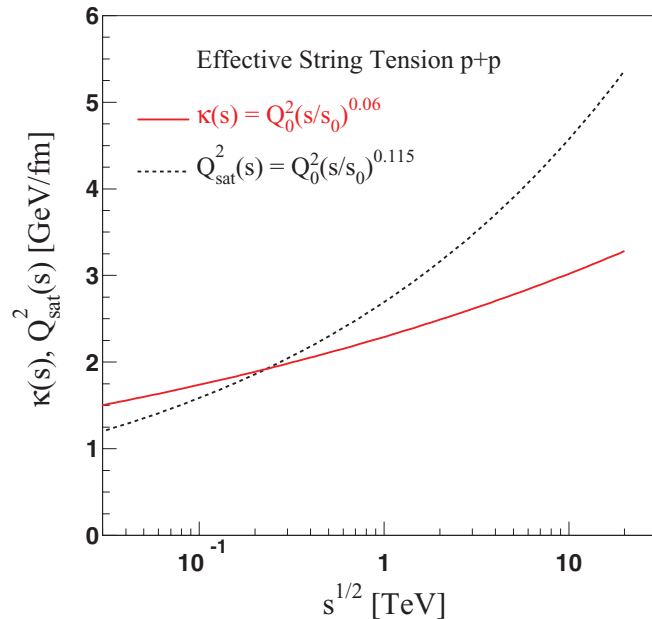


FIG. 1. (Color online) Energy dependence of the effective string tension  $\kappa(s)$  in  $pp$  collisions [Eq. (4)]. The values  $Q_{\text{sat}}^2$  [Eq. (3)] are from CGC model fits to LHC data from Ref. [29].

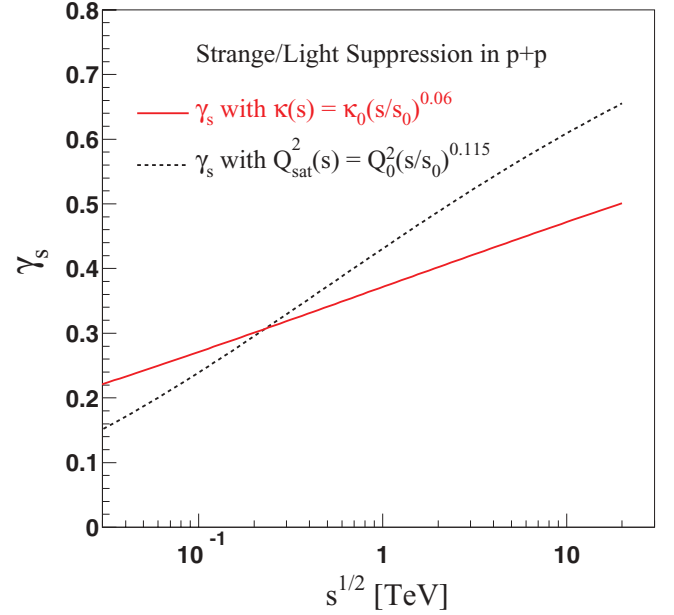


FIG. 2. (Color online) Energy dependence of the strange to light quark suppression factors,  $\gamma_s = s/u$ , using  $\kappa(s)$  from Eq. (4) and using  $Q_{\text{sat}}^2(s)$  from Ref. [29] are compared. (Note that this Schwinger suppression factor is not used in the CGC model.)

a strange quark compared to the normal suppression of strange quark ( $\gamma_s$ ),  $\gamma_{us} = [P(us\bar{u}\bar{s})/P(ud\bar{u}\bar{d})]/(\gamma_s)$ ; (iv) the suppression of spin-1 diquarks relative to spin-0 ones (apart from the factor of 3 enhancement of the former based on counting the number of spin states),  $\gamma_{10}$ ; and (v) the (anti-)quark ( $\sigma_q'' = \sqrt{\kappa/\kappa_0} \cdot \sigma_q$ ) and (anti-)diquark ( $\sigma_{qq}'' = \sqrt{\kappa/\kappa_0} \cdot f \cdot \sigma_{qq}$ ) Gaussian width. As an example we plot in Fig. 2 the energy dependence of the suppression factor  $\gamma_s = s/u$ , when the string tension values  $\kappa(s)$  are taken from Eq. (4) in comparison with the values predicted using  $Q_{\text{sat}}^2$  (Eq. (3) from the CGC model fit [29]).

The contributions of multiple jets to the multiplicity distributions in  $pp$  and  $p\bar{p}$  collisions have been studied in detail in Ref. [74]. Within the HIJING model, one assumes that nucleon-nucleon collisions at high energy can be divided into soft and hard processes with at least one pair of jet production with  $p_T > p_0$ . A cut-off scale  $p_0$  in the transverse momentum of the final jet production has to be introduced below which the interaction is considered nonperturbative and can be characterized by a finite soft parton cross section  $\sigma_{\text{soft}}$ . The inclusive jet cross section  $\sigma_{\text{jet}}$  at leading order (LO) [75] is

$$\sigma_{\text{jet}} = \int_{p_0^2}^{s/4} dp_T^2 dy_1 dy_2 \frac{1}{2} \frac{d\sigma_{\text{jet}}}{dp_T^2 dy_1 dy_2}, \quad (5)$$

where

$$\frac{d\sigma_{\text{jet}}}{dp_T^2 dy_1 dy_2} = K \sum_{a,b} x_1 f_a(x_1, p_T^2) x_2 f_b(x_2, p_T^2) \frac{d\sigma^{ab}(\hat{s}, \hat{t}, \hat{u})}{d\hat{t}} \quad (6)$$

depends on the parton-parton cross section  $\sigma^{ab}$  and parton distribution functions (PDF)  $f_a(x, p_T^2)$ . The summation runs over all parton species;  $y_1$  and  $y_2$  are the rapidities of the scattered partons;  $x_1$  and  $x_2$  are the light-cone momentum fractions carried by the initial partons. The factor  $K \approx 2$  accounts for the next-to-leading order (NLO) corrections to the leading order jet cross section. In the default HIJING model (v1.383), the Duke-Owens parametrization [76] of PDFs in nucleons is used. With the Duke-Owens parametrization of PDFs, an energy independent cut-off scale  $p_0 = 2 \text{ GeV}/c$  and a constant soft parton cross section  $\sigma_{\text{soft}} = 57 \text{ mb}$  are sufficient to reproduce the experimental data on total and inelastic cross sections and the hadron central rapidity density in  $p + p(\bar{p})$  collisions [51,52]. Our results have been obtained using the same set of parameters for hard scatterings as in the latest version of HIJING (v1.383).

### III. CHARGED PARTICLES

#### A. Charged hadron pseudorapidity

Charged hadron multiplicity measurements are the first results of the LHC physics program. Data for  $pp$  collisions were reported by the ALICE, ATLAS, and CMS collaborations [1–11]. The new data at midrapidity for non-single-diffractive interactions (NSD) and inelastic scattering (INEL) are shown in Fig. 3, which includes also similar results at lower energies. The main result is an observed sizable increase of the central pseudorapidity density with center-of-mass energy.

The main contribution to the multiplicity comes from soft interactions with only a small component originating from hard scattering of the partonic constituents of the proton. In contrast to the higher- $p_T$  regime, well described by pQCD, particle production in soft collisions is generally modeled phenomenologically to describe the different  $pp$

scattering processes: elastic scattering (el), single diffractive (SD), double diffractive dissociation (DD), and inelastic nondiffractive scattering (ND). Experimentally, minimum bias events are a close approximation of NSD interactions, i.e.,  $\sigma_{\text{NSD}} = \sigma_{\text{tot}} - \sigma_{\text{el}} - \sigma_{\text{SD}}$ , where  $\sigma_{\text{tot}}$  is the total cross section. The selection of NSD events is energy dependent and differs somewhat for different experimental triggers. The event selection of inelastic processes (INEL) includes SD interactions:  $\sigma_{\text{INEL}} = \sigma_{\text{tot}} - \sigma_{\text{el}}$ . The data therefore must be corrected for the SD component, involving model-dependent calculations.

The results of the model calculations for both NSD (left panel) and INEL (right panel) are also shown in Fig. 3. Solid lines depict results including the SCF effects, whereas the results without SCF effects are shown as dashed lines. Without SCF effects the model strongly overestimates the central charged particle density. The absolute value and energy increase of the central rapidity density are well reproduced assuming the energy-dependent string tension given in Eq. (4). At higher LHC energies (2.36 and 7 TeV), a discrepancy of 10–15% is observed.

As the colliding energy increases, the rate of multiple parton interactions (MPI) also increases, producing a rise in the central multiplicity. The increase with energy in our phenomenology is due to the interplay of the increased minijet production in high colliding energy with SCF effects. For an increase of strangeness suppression factors due to an increase of string tension with energy [ $\kappa = \kappa(s)$ ], the model predicts a decrease of produced pions due to energy conservation. Lower values of  $\kappa(s)$  imply smaller values for strangeness suppression factors, therefore a higher multiplicity of mesons (mostly pions).

Changing the effective value  $\kappa(s) = 2.89 \text{ GeV}/\text{fm}$  to  $\kappa(s) = 2.0 \text{ GeV}/\text{fm}$  results in an increased multiplicity of 11% at 7 TeV where the effect is greatest. In addition, the multiplicity

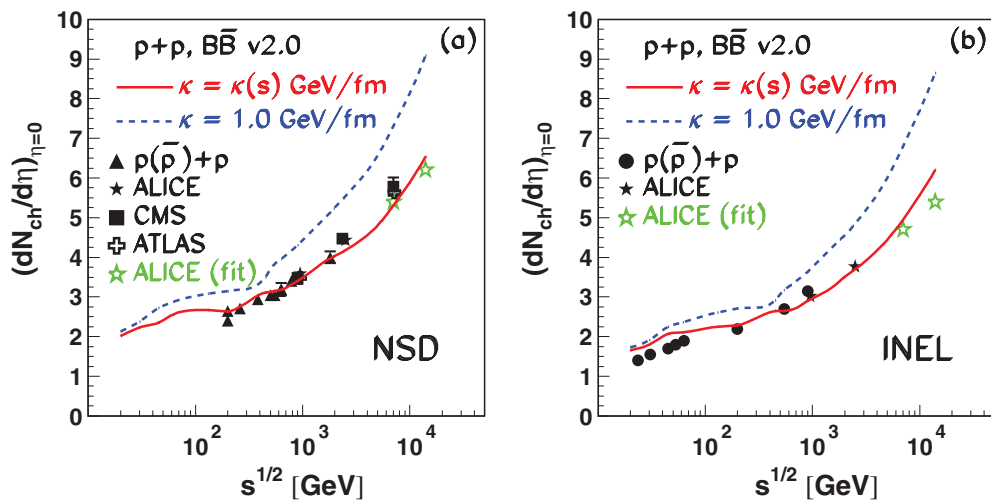


FIG. 3. (Color online) Comparison of HIJING/ $B\bar{B}$  (v2.0) predictions for central charged particle pseudorapidity density in  $pp$  and  $p\bar{p}$  interactions for non-single-diffractive (NSD) (left panel) and inelastic (INEL) (right panel) interactions as a function of center-of-mass energy. The solid and dashed lines are the results with and without SCF, respectively. The data are from Refs. [1–3,6,10,16–19,21] (left panel) and from Refs. [3,19,21,23] (right panel). Only statistical error bars are shown. The open stars at 7 and 14 TeV (ALICE fit) are obtained by a power law fit to lower-energy data from Refs. [6,34].

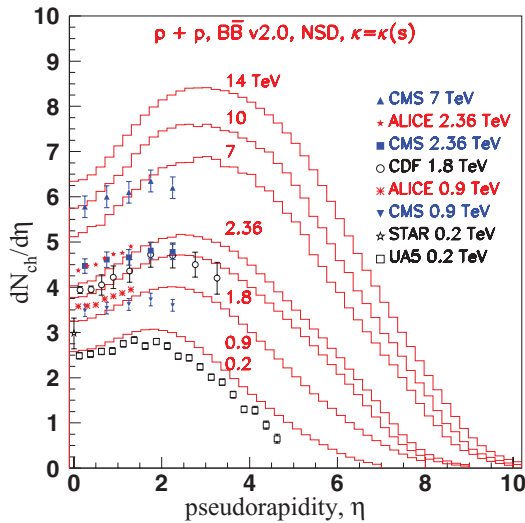


FIG. 4. (Color online) Comparison of HIJING/B $\bar{B}$  (v2.0) predictions for the pseudorapidity distribution of charged particles in  $p + p$  ( $\bar{p}$ ) collisions at various center-of-mass energies. The solid histograms are the results with SCF and  $JJ$  loops. The data are from Refs. [22] (UA5), [13] (STAR), [17] (CDF), [3,5] (ALICE), and [1,2] (CMS). Only statistical error bars are shown.

depends also on the value of the cut-off parameter  $p_0$ . Low values of  $p_0$  imply high rates of parton-parton scattering and hence high levels of particle multiplicity. Evidently for increasing values of  $p_0$  the opposite is expected. At 7 TeV, where the effect is also the largest, changing  $p_0$  by  $\pm 0.5$  GeV results in a change of only  $\mp 1.8\%$  for the central pseudorapidity density.

Data on the charged particle pseudorapidity distribution are also available over a limited  $\eta$  range [1–3,5,6]. These are presented in Fig. 4 where we also include results obtained at 0.2 TeV by the UA5 [22] and STAR [13] collaborations and with CDF results [17] obtained at the Tevatron for  $p\bar{p}$  collisions at 1.8 TeV. Consistent with the discussion above, a scenario with SCF effects (solid histograms) reproduces the measured multiplicity distributions well. At all energies considered, theoretical calculations predict a central dip at midrapidity that is consistent with the observations. At 0.9 and 2.36 TeV, the shape of the distribution measured by the ALICE collaboration is very well reproduced, while the CMS results show a much flatter distributions than calculated (also the case at 7 TeV). Data over a larger rapidity range are needed to determine the shape of the falling density in the fragmentation region. For completeness, predictions at 10 and 14 TeV, the higher LHC energies, are also shown.

### B. Transverse-momentum spectra

The measured transverse-momentum distributions for NSD events over an energy range  $\sqrt{s} = 0.63$ –7 TeV are shown in Fig. 5. These recent measurements are performed in the central rapidity region and cover a wide  $p_T$  range ( $0.15 < p_T < 10$  GeV/ $c$ ), where both hard and soft processes are expected to contribute. The data of ATLAS and CMS

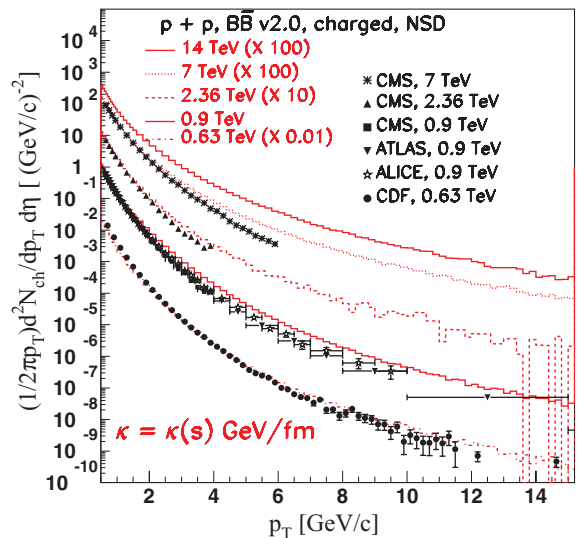


FIG. 5. (Color online) Comparison with data of HIJING/B $\bar{B}$  (v2.0) predictions of charged-hadron transverse-momentum distributions at LHC energies. The calculated spectra include the combined effects of SCF and  $JJ$  loops. The histograms and data have been scaled for clarity by the factors indicated. The data are from Refs. [77] (CDF), [4] (ALICE), [7] (ATLAS), and [1,2] (CMS). Error bars include only the statistical uncertainties.

are measured in larger pseudorapidity intervals ( $|\eta| < 2.5$ ). In contrast, ALICE and CDF measurements are in a very central region ( $|\eta| < 0.8$  and  $|\eta| < 1.0$ , respectively). The calculation takes into account the difference in acceptance, but, as can be concluded from Fig. 4, this difference in pseudorapidity range has a negligible effect on the measured cross section.

The model calculations, including SCF effects, describe the data well at  $\sqrt{s} = 0.63$  TeV, but lead to a harder spectrum that observed at higher energy. The model gives a fair description of the spectral shape at low  $p_T$  but overestimates the data at high  $p_T$ . The discrepancy is highest (up to a factor of three) at  $\sqrt{s} = 7$  TeV. We do not understand the source of this discrepancy and await higher  $p_T$  data to draw a firm conclusion. However, in our phenomenology this could indicate that jet quenching, i.e., suppression of high- $p_T$  particles like that observed at RHIC energies in nucleus-nucleus collisions, could also appear in  $pp$  collisions in events with large multiplicity. This overestimation of high  $p_T$  yield leads also to a similar overestimation of the mean transverse momentum ( $\langle p_T \rangle$ ) and of the correlation of mean  $\langle p_T \rangle$  as a function of  $N_{ch}$ , which we do not discuss here.

Within our model we generate events with different numbers of minijets up to some maximum values. High numbers of minijets lead to higher multiplicity events. For events with ten minijets (the maximum assumed in our calculation), the central charged particle pseudorapidity density could increase up to  $\approx 20$  and the total multiplicity could be greater than 150 at Tevatron energy (1.8 TeV). The measurements of two-particle correlations over the entire azimuth could reveal the jet structure related to high- $p_T$  particles [78]. The study of these correlations in events with high multiplicity could help us to draw a firm conclusion with regard to a possible jet-quenching phenomenon in  $pp$  collisions.

## IV. IDENTIFIED PARTICLE SPECTRA AND RATIOS

### A. Baryon-to-meson ratio

The  $pp$  single-particle inclusive  $p_T$  spectra measurements are important for understanding collision dynamics, since the various particles show different systematic behavior, as observed at RHIC energy [78]. Detailed theoretical predictions for single inclusive hadron production (including strange hyperons) are discussed in this section. Baryon-to-meson ratios ( $B/M$ ) are experimental observables that can be used at the LHC for investigating multiparton interactions and helping to understand the underlying physics [79–81].

Unexpectedly high  $B/M$  ratios observed in  $A + A$  collisions have been discussed in terms of recombination and coalescence mechanisms [82–84]. Such high ratios at intermediate  $p_T$  were also reported in  $pp$  collisions at RHIC [85] and at the Tevatron [86]. In  $pp$  collisions, however, a coalescence/hadronization scenario is not favored due to low-phase-space density in the final state. Our HIJING/ $\bar{B}\bar{B}$  model, with SCF effects included, provides an alternative dynamical explanation of the heavy-ion data at RHIC energies. We have shown that the model also predicts an increasing yield of (multi-)strange particles, thereby better describing the experimental data [64].

Figure 6(b) shows a comparison of model predictions with CDF experimental data [86] of the strange baryon-to-meson ratio  $(\Lambda^0 + \bar{\Lambda}^0)/K_S^0$  at 1.8 TeV. The particle  $p_T$  spectra are shown in Fig. 6(a). The measured ratio is fairly well described within our phenomenology. The larger string tension parametrization results in a predicted increase of the ratio  $(\Lambda^0 + \bar{\Lambda}^0)/K_S^0$  by a factor of  $\approx 10$  at the Tevatron energy. The  $p_T$  spectra show that the increased ratio is due almost entirely to an increase of the  $\Lambda$  cross section that is well described with  $\kappa(s) = \kappa_0 (s/s_0)^{0.06}$  GeV/fm. The model underestimates the kaon production by 15–25%.

The model predictions at 7 TeV, currently the maximum energy where there are data [87], are shown in Fig. 7(b). The model gives a good description of hyperon production

( $\Lambda^0 + \bar{\Lambda}^0$ ), for which an increase by a factor of 10 is still predicted if SCF effects are considered. However, our calculations underestimate by approximately a factor of 2 the yield of  $K_S^0$  and, as a consequence, result in a higher ratio than that observed. This result needs further investigation (theoretical and experimental) on heavy-flavor production at this energy. We note that the models PYTHIA [88,89] and energy-conserving partons off-shell remnants and splitting of partons ladders (EPOS) [90,91] cannot reproduce the observed high  $B/M$  ratio (see Figs. 6 and 7 from Ref. [80]). The preliminary data reported by the CMS collaboration indicate high hyperon yield. Comparisons with PYTHIA results show that this model significantly underestimates the hyperon yields in  $pp$  collisions at 0.9 and 7 TeV [87].

The strange particle ratios could also be the manifestation of new collective phenomena. In the EPOS model such an increase is obtained if the production of a *miniplasma* is considered in  $pp$  collisions [24,91]. If confirmed by future measurements, the study of these observables could open a perspective on new physics in  $pp$  interactions.

Similar conclusions are obtained from the study of the proton/pion ( $p/\pi^+$ ,  $\bar{p}/\pi^-$ ) ratios where data exist at lower energies [92,93]. These data, shown in Fig. 8, are limited to low  $p_T < 2$  GeV/c. Adding SCF effects results in a very sizable increase of the ratio and our calculations provide a good description of the data in the measured range. However, as the calculations indicate, to draw a final conclusion measurements at intermediate and high  $p_T$  are needed.

To the extent that the LHC experiments are able to identify hadron species, such data will provide vital input to validate this interpretation. The model predictions at LHC energies for the  $p_T$  dependence of the  $\bar{p}/\pi^-$  ratio are shown in Fig. 9. An enhancement up to the highest LHC energy and a weak energy dependence, with a saturation that sets in for a center-of-mass energy  $\sqrt{s} > 2.36$  TeV, is predicted. Note that preliminary data at 0.9 TeV reported by the ALICE collaboration for  $p_T$  spectra of pions ( $\pi^+$ ) and protons ( $p$ ) [94] cover to  $p_T < 2.5$  GeV/c. The model results, with SCF effects included

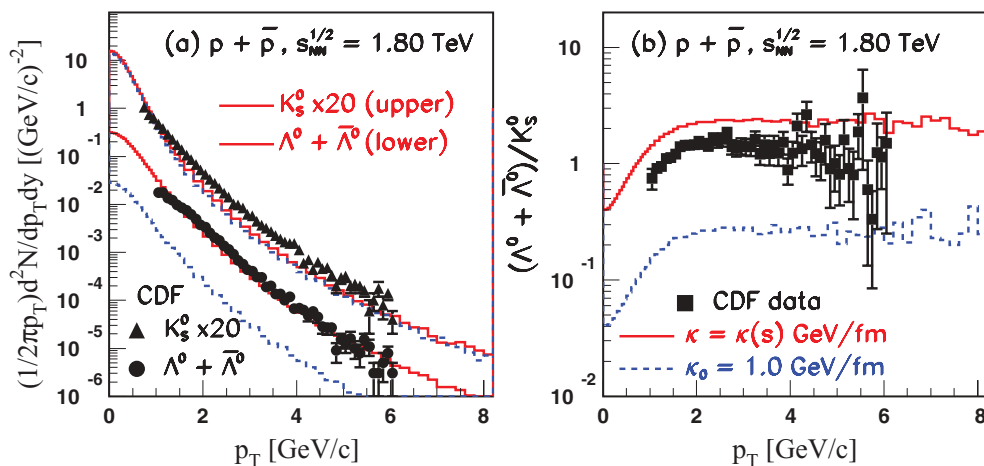


FIG. 6. (Color online) HIJING/ $\bar{B}\bar{B}$  (v2.0) predictions at  $\sqrt{s} = 1.8$  TeV of baryon and mesons transverse momentum at midrapidity ( $-1 < y < 1$ ) (a) and their ratios for single strange particles  $(\Lambda^0 + \bar{\Lambda}^0)/K_S^0$  (b) in minimum bias  $p\bar{p}$  collisions. The solid and dashed lines have the same meaning as in Fig. 3. Experimental results at  $\sqrt{s} = 1.8$  TeV are from Ref. [86] (CDF Collaboration). Error bars include only the statistical uncertainties. The ratios (b) have been calculated by us, dividing the spectra in (a).

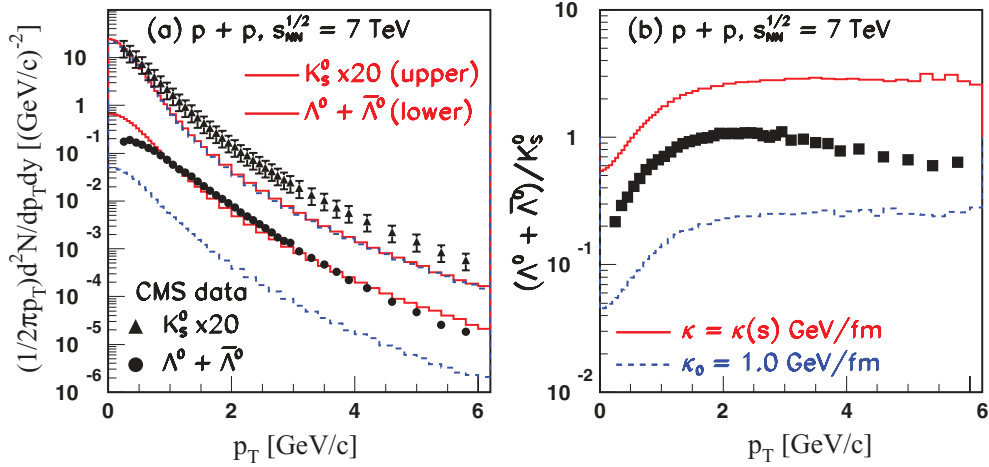


FIG. 7. (Color online) Predictions of the HIJING/B $\bar{B}$  (v2.0) model for baryon and meson transverse momentum in the rapidity range  $-2 < y < 2$  (a) and their ratio (b) for minimum bias  $p\bar{p}$  collisions at  $\sqrt{s} = 7.0$  TeV. The solid and dashed lines have the same meaning as in Fig. 3. The experimental results (a) are from Ref. [87] (CMS Collaboration). Error bars include only the statistical uncertainties. The ratios (b) have been calculated by us, dividing the spectra in (a).

(dot-dashed histogram in Fig. 9) are consistent with a  $p/\pi^+$  ratio derived from the spectra reported by ALICE at 0.9 TeV in Ref. [94].

In our approach, the dynamical mechanism that leads to such high values of  $B/M$  ratios is SCF appearing at the initial stage of the interaction. The SCF mechanism strongly modifies the fragmentation processes (strangeness suppression factors) and thus results in a huge increase of (strange) baryons. This interpretation is also supported by more sophisticated theoretical calculations, in a scenario in which a time-dependent pulse for the initial strength of the color field is considered [95,96]. The large enhancement of the baryon-to-meson ratios demonstrates that SCF could play an important role in multiparticle production in  $pp$  collisions at LHC energies and that high-energy density fluctuations

can reach very high densities, potentially comparable to those reached in central Au + Au collisions at RHIC energies [97].

### B. Baryon-antibaryon asymmetry

From the study of the baryon-antibaryon asymmetry one can learn about the mechanism of baryon number transport. Baryon production via the conventional default quark-diquark mechanisms in the Lund string model are known to be inadequate even in  $e^+ + e^-$  phenomenology. This is one of the main reasons for our continued exploration of alternative baryon junction mechanisms. The details of the new implementation of  $J\bar{J}$  loops in HIJING/B $\bar{B}$  (v2.0) are described in Ref. [64] Sec II A. In HIJING/B $\bar{B}$  (v2.0) the main two mechanisms

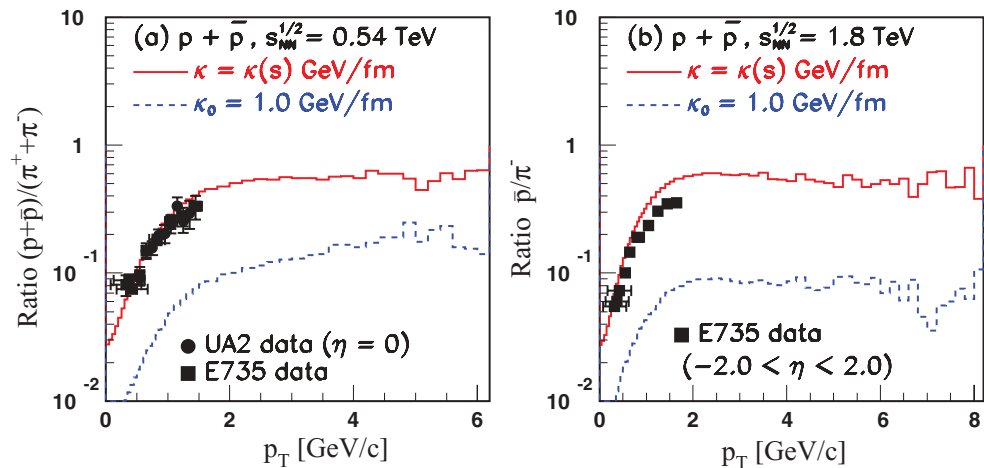


FIG. 8. (Color online) Comparison of HIJING/B $\bar{B}$  (v2.0) predictions with data on the nonstrange baryon-over-meson ratios from minimum bias events in the rapidity range  $|y| < 2$ . The solid and dashed lines have the same meaning as in Fig. 3. Experimental results for  $|y| < 2$  at  $\sqrt{s} = 0.54$  TeV (left panel) and at  $\sqrt{s} = 1.8$  TeV (right panel) are from Ref. [92] (E735 Collaboration). The results at midrapidity at  $\sqrt{s} = 0.54$  TeV (left panel) are from Ref. [93] (UA2 Collaboration). Error bars include only the statistical uncertainties.

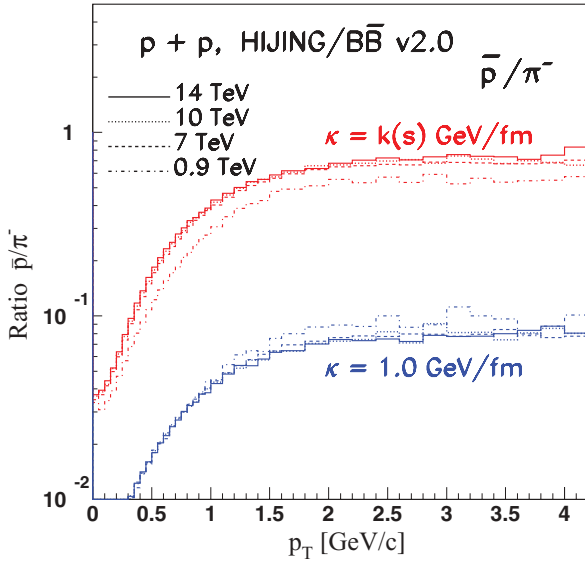


FIG. 9. (Color online) Predictions of the HIJING/B $\bar{B}$  (v2.0) model of nonstrange baryon over meson ratios ( $\bar{p}/\pi^-$ ) for minimum bias events at midrapidity at LHC energies. The upper curves correspond to calculations which include the effects of SCF and  $J\bar{J}$  loops. The lower curves corresponds to calculations without SCF effects. The results are at 0.9 TeV (dot-dashed histograms), at 7 TeV (dashed histograms), at 10 TeV (dotted histograms), and at 14 TeV (solid histograms).

for baryon production are quark-diquark ( $q$ - $qq$ ) string fragmentation and  $J\bar{J}$  loops [68] in which baryons are produced approximately in pairs. In a junction loop a color flux line splits at some intermediate point into two flux lines at one junction and then the flux lines fuse back at an antijunction somewhere further along the original flux line. The distance in rapidity between these points is chosen via a Regge distribution [64]. We assume that, from the non-single-diffractive nucleon-nucleon ( $NN$ ) interaction cross section ( $\sigma_{\text{NSD}}$ ), a fraction

$f_{J\bar{J}} = \sigma_{J\bar{J}}/(\sigma_{\text{INEL}} - \sigma_{\text{SD}})$  of the events excite a junction loop. The probability that the incident baryon has a  $J\bar{J}$  loop in  $p(A) + A$  collisions after  $n_{\text{hits}}$  simulated binary collisions is given by

$$P_{J\bar{J}} = 1 - (1 - f_{J\bar{J}})^{n_{\text{hits}}}, \quad (7)$$

where  $\sigma_{J\bar{J}} = 17$  mb,  $\sigma_{\text{SD}}$  is parametrized in the model, and the total inelastic nucleon-nucleon cross sections are calculated [42]. These cross sections imply that a junction loop occurs in  $pp$  collisions with a rather high probability (at RHIC energy  $f_{J\bar{J}} \approx 0.5$  for  $\sigma_{\text{INEL}} = 42$  mb). Taking a constant value for  $\sigma_{J\bar{J}}$  results in a decrease with energy of the probability  $P_{J\bar{J}}$  due to a faster increase with energy of  $\sigma_{\text{INEL}}$  relative to  $\sigma_{\text{SD}}$ . The actual probability is modified also by string fragmentation processes for which we consider a threshold cutoff mass  $M_c = 6$  GeV/ $c^2$  in order to have enough kinematic phase space to produce  $B\bar{B}$  pairs. We have investigated the sensitivity of the results to the value of parameters  $\sigma_{J\bar{J}}$  and  $M_c$  and found no significant variation on pseudorapidity distributions of charged particles for  $15 \text{ mb} < \sigma_{J\bar{J}} < 25 \text{ mb}$  and for  $4 \text{ GeV}/c^2 < M_c < 6 \text{ GeV}/c^2$ .

Baryon number transport is quantified in terms of the rapidity loss ( $\delta y_{\text{loss}} = \delta y_{\text{beam}} - \delta y_{\text{baryon}}$ , where  $y_{\text{beam}}$  and  $y_{\text{baryon}}$  are the rapidity of incoming beam and outgoing baryon, respectively) and has been discussed within our model phenomenology for  $A + A$  collisions in Refs. [63–65]. It was shown that HIJING/B $\bar{B}$  (v1.0) overestimate the stopping power and give a mild energy dependence of net baryons at midrapidity. The energy dependence of net baryons at midrapidity per participant pair within HIJING/B $\bar{B}$  (v2.0) is proportional to  $(s/s_0)^{-1/4+\Delta/2}$ , similar to the dependence predicted in Ref. [98], with the assumption that  $J\bar{J}$  is the dominant mechanism. This dependence is obtained assuming the following parameters [65]:  $s_0 = 1 \text{ GeV}^2$  (the usual parameter of Regge theory),  $\alpha(0) = 1/2$  (the reggeon intercept of the trajectory), and  $\alpha_P(0) = 1 + \Delta$  (where  $\Delta \approx 0.01$ ) for the pomeron intercept.

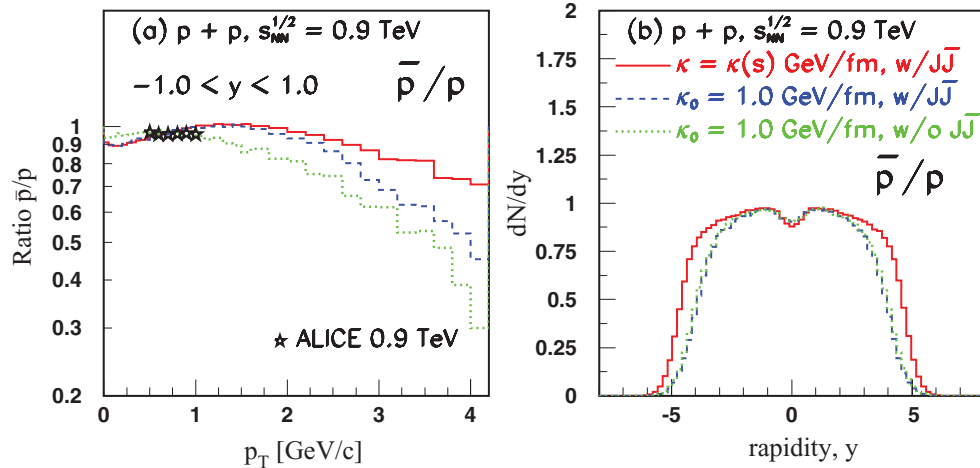


FIG. 10. (Color online) HIJING/B $\bar{B}$  (v2.0) predictions  $p_T$  distributions (a) at midrapidity for the  $\bar{p}/p$  ratio at  $\sqrt{s} = 0.9$  TeV; rapidity distributions are shown in (b). The results are from three possible scenarios: without contributions from SCF and  $J\bar{J}$  loops (dotted histograms), including only the effect of  $J\bar{J}$  loops (dashed histograms) and including both effects (SCF and  $J\bar{J}$  loops) (solid histograms). The data are from Ref. [99] (ALICE Collaboration). Only statistical errors are shown.

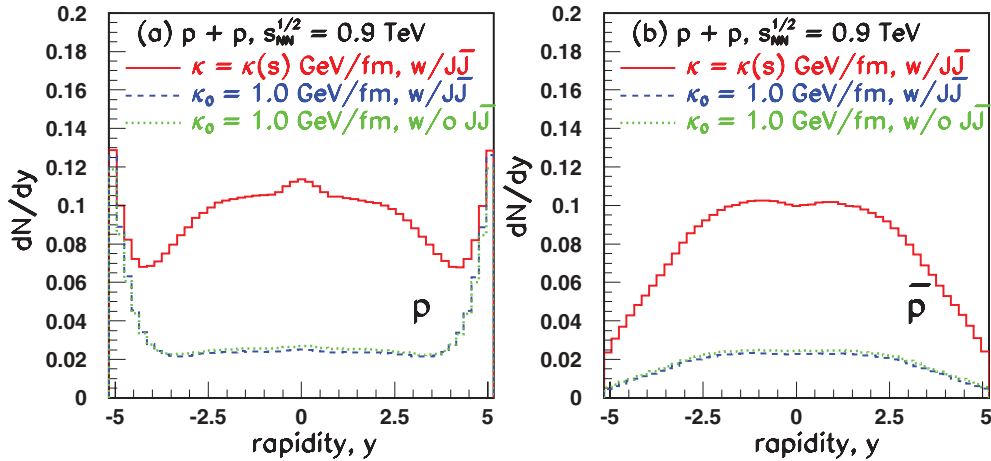


FIG. 11. (Color online) Predictions of the HIJING/BĪ (v2.0) model for rapidity distributions of protons (a) and antiprotons (b) at  $\sqrt{s} = 0.9$  TeV. The histograms have the same meaning as in Fig. 10.

Recently, the ALICE Collaboration reported results [99] on midrapidity antiproton-to-proton ratio in  $pp$  collisions at  $\sqrt{s} = 0.9$  and 7 TeV and equivalently the proton-antiproton asymmetry,  $A = (N_p - N_{\bar{p}})/(N_p + N_{\bar{p}})$ . These data could be used to constrain Regge inspired model descriptions of baryon asymmetry. The authors state that, within statistical errors, the observed  $\bar{p}/p$  ratio shows no dependence on transverse momentum or rapidity in the limited measured acceptance ( $-0.8 < y < 0.8$ ;  $0 < p_T < 1$  GeV/c). In Fig. 10(a) are compared the HIJING/BĪ (v2.0) model predictions with the published data at 0.9 TeV. Our model predicts negligible dependence on  $p_T$  for  $0 < p_T < 2$  GeV/c and a slight  $p_T$  dependence at higher  $p_T$  where both effects ( $J\bar{J}$  loops and SCF) could contribute. The full calculation is shown by the solid histogram. The dotted line is the prediction without  $J\bar{J}$  loops and SCF effects while the dashed line includes the effect of  $J\bar{J}$  loops only. Over the measured ranges the rapidity distribution of the ratio  $\bar{p}/p$  distribution is not sensitive to the various scenarios presented. The scenario with combined effects results in a wider rapidity distribution at  $y > 3$  [Fig. 10(b)]. The narrow structure observed near  $y = 0$  has no physical significance and we believe that it is likely due to a numerical artifact of our current implementation of fragmentation scheme.

Separate proton and antiproton rapidity distributions are, however, much more sensitive to SCF effects, as seen in Fig. 11. The model predicts a substantial increase (by a factor of  $\approx 5$ ) for  $p(\bar{p})$ , when SCF are taken into account. Due to the high cutoff mass  $M_c = 6$  GeV/c<sup>2</sup> the effect of  $J\bar{J}$  loops is very small over the entire rapidity region. Analysis of the 7-TeV data leads to similar conclusions but shows less effect at high  $p_T$ .

Over the measured range the feed-down-corrected data for the  $\bar{p}/p$  ratio rises from  $0.957 \pm 0.006$  at 0.9 TeV to  $0.99 \pm 0.005$  at 7 TeV [99]. Although the measured midrapidity ratio is close to unity there is a small but significant excess of protons over antiprotons corresponding to an asymmetry of  $A = 0.022 \pm 0.003$  and  $A = 0.005 \pm 0.003$  at  $\sqrt{s} = 0.9$  and 7 TeV, respectively. Within our model using a Regge

intercept of  $\alpha_0 = 1/2$  results in a proton-antiproton asymmetry  $A_{\text{model}} = 0.032$  (0.002) at 0.9 TeV (7 TeV). The result overestimates the value of asymmetry at 0.9 TeV. These values show that a fraction of the baryon number associated with the beam particles is transported over rapidity intervals of less than seven units. However, a better understanding of the baryon transport would require measuring the rapidity dependence of the asymmetry over a larger range.

In Ref. [64] we discuss the predicted rapidity correlation length for production of baryon-antibaryon pairs within our model. The predicted rapidity correlation length  $[1 - \alpha(0)]^{-1}$  depends on the value of the Regge intercept  $\alpha(0)$  [43]. A value of  $\alpha(0) \simeq 0.5$  leads to rapidity correlations in the range  $|y_B - y_{\bar{B}}| \sim 2$ , while a value  $\alpha(0) \simeq 1.0$  [100] is associated with infinite range rapidity correlations. This kind of analysis and future measurements at LHC energies will help us to determine better the specific parameters characterizing  $J\bar{J}$  loops used in the calculations of baryon number transport and/or baryon-antibaryon asymmetry while helping to establish the validity of Regge inspired models.

## V. SUMMARY AND CONCLUSIONS

We have studied the influence of strong longitudinal color fields and of possible multi-gluon dynamics (gluon junctions) in particle production in  $pp$  collisions, with a focus on RHIC, to Tevatron, and LHC energies. We have investigated a set of observables sensitive to the dynamics of the collisions, covering both longitudinal and transverse degree of freedom. A detailed comparison with newly available experimental data from the LHC has been performed.

We found that the inclusion of the multiple minijet source limits the growth of the string tension  $\kappa(s)$  to be approximately only linear as a function of saturation scale  $Q_{\text{sat}}$  [Eq. (4)], in contrast to recent approaches [29] where  $\kappa(s)$  scales as  $Q_{\text{sat}}^2$  [Eq. (3)]. The reason for this is that in the CGC model the collinear factorized minijet mechanism is suppressed by geometric scaling to much higher  $p_T$ . Future measurements

at LHC energies ( $\sqrt{s} = 7$  and  $14$  TeV), extended to high  $p_T$ , will help to clarify the validity of this mechanism.

We have shown that SCF could play an important role in particle production at midrapidity in  $pp$  collisions. Our calculations show that high-energy density fluctuations in  $pp$  collisions at LHC can reach densities comparable to those reached in central nuclear ( $A + A$ ) collisions at RHIC. A large enhancement of the (strange) baryon-to-meson ratios that persists up to the highest LHC energy can be explained as an effect of SCF that appears at the initial stage of the interaction. The mechanisms of hadron production are very sensitive to the early phase of the collisions, when fluctuations of the color field strength are highest. SCF effects are modeled by varying the effective string tension that controls the  $q\bar{q}$  and  $qq\bar{q}\bar{q}$  pair creation rates and strangeness suppression factors. SCF, therefore, may modify the fragmentation processes with a resultant huge increase of (strange) baryons.

We show that both  $J\bar{J}$  loops and SCF effects could play an important role in baryon (antibaryon) production at midrapidity in  $pp$  collisions at LHC energies. Introducing a new  $J\bar{J}$  loop algorithm in the framework of HIJING/B $\bar{B}$  (v2.0) leads to a consistent and significant improvement in the description of the recent experimental results for proton-antiproton and for baryon-antibaryon asymmetry in comparison to the older versions HIJING/B or HIJING/B $\bar{B}$  (v1.0) [43]. We have shown that baryon number transport is suppressed for  $\delta y > 7$ , a result that is confirmed by recent ALICE measurements [99].

The present study is limited to the effect of initial-state baryon production via possible junction dynamics in strong fields. It would be very useful to consider a generalization of

back reaction effects [58] to the case not only of pair production relevant for mesons but to the more difficult three string junction configurations needed to describe baryon production.

A greater sensitivity to SCF effects is expected also for open charm and bottom production [66]. In particular, measurements of rapidity and  $p_T$  distributions for particles involving charm and bottom quark would provide an important test of the relevance of SCF fluctuations, helping us to determine values of the suppression factors  $\gamma_{Q\bar{Q}}$  (where  $Q = qq, s, c, b$ ), which have strong dependence on the main parameters of QCD (the constituent and current quark masses) and on the system size. Even though the success of this procedure has been clearly illustrated here, a fuller understanding of particle production and especially of (multi-)strange particles in ultrarelativistic  $pp$  collisions at the LHC remains an exciting open question and will continue to challenge many theoretical ideas.

## ACKNOWLEDGMENTS

We thank S. Das Gupta and S. Jeon for useful discussions and continued support. We thank P. Levai for helpful discussions and suggestions throughout this project. V.T.P. acknowledges computer facilities at Columbia University, New York, where part of these calculations were performed. This work was supported by the Natural Sciences and Engineering Research Council of Canada. This work was also supported by the Division of Nuclear Science, of the US Department of Energy under Contracts No. DE-AC03-76SF00098 and No. DE-FG02-93ER-40764.

- 
- [1] V. Khachatryan *et al.* (CMS Collaboration), *J. High Energy Phys.* **02** (2010) 041.
- [2] V. Khachatryan *et al.* (CMS Collaboration), *Phys. Rev. Lett.* **105**, 022002 (2010).
- [3] K. Aamodt *et al.* (ALICE Collaboration), *Eur. Phys. J. C* **65**, 111 (2010).
- [4] K. Aamodt *et al.* (ALICE Collaboration), *Phys. Lett. B* **693**, 53 (2010).
- [5] K. Aamodt *et al.* (ALICE Collaboration), *Eur. Phys. J. C* **68**, 345 (2010).
- [6] K. Aamodt *et al.* (ALICE Collaboration), *Eur. Phys. J. C* **68**, 89 (2010).
- [7] G. Aad *et al.* (ATLAS Collaboration), *Phys. Lett. B* **688**, 21 (2010).
- [8] G. Aad *et al.* (ATLAS Collaboration), CERN Report ATLAS-CONF-201-024 (2010) (unpublished).
- [9] G. Aad *et al.* (ATLAS Collaboration), CERN Report ATLAS-CONF-201-031 (2010) (unpublished).
- [10] G. Aad *et al.* (ATLAS Collaboration), CERN Report ATLAS-CONF-201-046 (2010) (unpublished).
- [11] G. Aad *et al.* (ATLAS Collaboration), CERN Report ATLAS-CONF-201-047 (2010) (unpublished).
- [12] G. Aad *et al.* (ATLAS Collaboration), [arXiv:1012.5104](https://arxiv.org/abs/1012.5104) [hep-ex] (submitted to New J. of Phys.).
- [13] B. I. Abelev *et al.* (STAR Collaboration), *Phys. Rev. C* **79**, 034909 (2009).
- [14] T. Aaltonen *et al.* (CDF Collaboration), *Phys. Rev. D* **79**, 112005 (2009).
- [15] T. Alexopoulos *et al.* (E735 Collaboration), *Phys. Lett. B* **336**, 599 (1994).
- [16] C. Albajar *et al.* (UA1 Collaboration), *Nucl. Phys. B* **335**, 261 (1990).
- [17] F. Abe *et al.* (CDF Collaboration), *Phys. Rev. D* **41**, 2330 (1990).
- [18] R. E. Ansorge *et al.* (UA5 Collaboration), *Z. Phys. C* **43**, 357 (1989).
- [19] R. E. Ansorge *et al.* (UA5 Collaboration), *Z. Phys. C* **37**, 191 (1988).
- [20] F. Abe *et al.* (CDF Collaboration), *Phys. Rev. Lett.* **61**, 1819 (1988).
- [21] G. J. Alner *et al.*, *Phys. Rep.* **154**, 247 (1987).
- [22] R. E. Ansorge *et al.* (UA5 Collaboration), *Z. Phys. C* **33**, 175 (1986).
- [23] W. Thome *et al.*, *Nucl. Phys. B* **129**, 365 (1977).
- [24] N. Armesto *et al.*, *J. Phys. G* **35**, 054001 (2008).
- [25] N. Armesto, in *Quark Gluon Plasma 4*, edited by R. C. Hwa and X.-N. Wang (World Scientific, Singapore, 2010), p. 375.
- [26] M. Mitrovski, T. Schuster, G. Graf, H. Petersen, and M. Bleicher, *Phys. Rev. C* **79**, 044901 (2009).
- [27] E. Levin and A. H. Rezaeian, *Phys. Rev. D* **82**, 014022 (2010).
- [28] E. Levin and A. H. Rezaeian, *Phys. Rev. D* **82**, 054003 (2010).
- [29] L. McLerran and M. Praszalowicz, *Acta Phys. Pol. B* **41**, 1917 (2010).

- [30] C. Merino, C. Pajares, M. M. Ryzhinskiy, and Yu. M. Shabelski, [arXiv:1007.3206](#) [hep-ph].
- [31] P. Z. Skands, *Phys. Rev. D* **82**, 074018 (2010).
- [32] A. Buckley, H. Hoeth, H. Schulz, and J. E. von Seggern, *PoS ACAT08*, 112 (2009).
- [33] A. Moraes, C. Buttar, and I. Dawson, *Eur. Phys. J. C* **50**, 435 (2007).
- [34] J. F. Grosse-Oetringhaus and K. Reyggers, *J. Phys. G* **37**, 083001 (2010).
- [35] I. Kraus, J. Cleymans, H. Oeschler, and K. Redlich, *Phys. Rev. C* **79**, 014901 (2009).
- [36] A. B. Kaidalov and M. G. Poghosyan, *Eur. Phys. J. C* **67**, 397 (2010).
- [37] E. K. G. Sarkisyan and A. S. Sakharov, *Eur. Phys. J. C* **70**, 533 (2010).
- [38] A. Warburton (CDF and D0 Collaborations), *PoS HCP2009*, 013 (2009).
- [39] M. H. Seymour, to appear in the Proceedings of Physics at LHC 2010 (PHLC2010), 7–12 June 2010, Hamburg Germany, [arXiv:1008.2927](#) [hep-ph].
- [40] R. Sassot, P. Zurita, and M. Stratmann, *Phys. Rev. D* **82**, 074011 (2010).
- [41] W. T. Deng, X. N. Wang, and R. Xu, [arXiv:1008.1841](#) [hep-ph].
- [42] X. N. Wang and M. Gyulassy, *Comput. Phys.* **83**, 307 (1994); X. N. Wang, *Phys. Rep.* **280**, 287 (1997).
- [43] S. E. Vance and M. Gyulassy, *Phys. Rev. Lett.* **83**, 1735 (1999).
- [44] B. Andersson, G. Gustafson, and B. Nilsson-Almqvist, *Nucl. Phys. B* **281**, 289 (1987).
- [45] A. Capella *et al.*, *Phys. Rep.* **236**, 225 (1994).
- [46] T. S. Biro, H. B. Nielsen, and J. Knoll, *Nucl. Phys. B* **245**, 449 (1984).
- [47] M. Gyulassy and A. Iwazaki, *Phys. Lett. B* **165**, 157 (1985).
- [48] F. Gelis, T. Lappi, and L. McLerran, *Nucl. Phys. A* **828**, 149 (2009); T. Lappi and L. McLerran, *ibid.* **772**, 200 (2006).
- [49] L. McLerran, *J. Phys. G* **35**, 104001 (2008).
- [50] T. Sjostrand, *Comput. Phys. Commun.* **82**, 74 (1994).
- [51] X. N. Wang and M. Gyulassy, *Phys. Rev. D* **44**, 3501 (1991).
- [52] X. N. Wang and M. Gyulassy, *Phys. Rev. D* **45**, 844 (1992).
- [53] P. Levai and B. Muller, *Phys. Rev. Lett.* **67**, 1519 (1991).
- [54] T. Pierog, S. Porteboeuf, I. Karpenko, and K. Werner, to appear in the Proceedings of 45th Rencontre de Moriond, QCD and High Energy Interactions, 13–20 March 2010, La Thuile, Aosta Valley, Italy, [arXiv:1005.4526](#) [hep-ph].
- [55] A. Iwazaki, [arXiv:0904.1449](#) [hep-ph].
- [56] J. S. Schwinger, *Phys. Rev.* **82**, 664 (1951).
- [57] D. Kharzeev, E. Levin, and K. Tuchin, *Phys. Rev. C* **75**, 044903 (2007).
- [58] N. Tanji, *Ann. Phys.* **324**, 1691 (2009).
- [59] R. Ruffini, G. Vereshchagin, and S. S. Xue, *Phys. Rep.* **487**, 1 (2010).
- [60] N. Tanji, *Ann. Phys.* **325**, 2018 (2010).
- [61] T. D. Cohen and D. A. McGady, *Phys. Rev. D* **78**, 036008 (2008).
- [62] F. Hebenstreit, R. Alkofer, and H. Gies, *Phys. Rev. D* **78**, 061701 (2008).
- [63] V. Topor Pop, M. Gyulassy, J. Barrette, and C. Gale, *Phys. Rev. C* **72**, 054901 (2005).
- [64] V. Topor Pop, M. Gyulassy, J. Barrette, C. Gale, S. Jeon, and R. Bellwied, *Phys. Rev. C* **75**, 014904 (2007), and references therein.
- [65] N. Armesto *et al.*, *J. Phys. G* **35**, 054001 (2008); V. Topor Pop *et al.*, *ibid.* **35**, 15 (2008); **35**, 57 (2008).
- [66] V. Topor Pop, J. Barrette, and M. Gyulassy, *Phys. Rev. Lett.* **102**, 232302 (2009).
- [67] V. Topor Pop, M. Gyulassy, J. Barrette, C. Gale, X. N. Wang, and N. Xu, *Phys. Rev. C* **70**, 064906 (2004).
- [68] G. Ripka, ed., *Dual Superconductor Models of Color Confinement*, Lecture Notes in Physics, Vol. 639 (Springer-Verlag, Berlin, 2004), p. 138.
- [69] M. Cristoforetti, P. Faccioli, G. Ripka, and M. Traini, *Phys. Rev. D* **71**, 114010 (2005).
- [70] K. Nakamura *et al.* (Particle Data Group), *J. Phys. G* **37**, 075021 (2010).
- [71] N. S. Amelin, N. Armesto, C. Pajares, and D. Sousa, *Eur. Phys. J. C* **22**, 149 (2001).
- [72] L. V. Gribov, E. M. Levin, and M. G. Ryskin, *Phys. Rep.* **100**, 1 (1983).
- [73] G. Altarelli and G. Parisi, *Nucl. Phys. B* **126**, 298 (1977).
- [74] X. N. Wang, *Phys. Rev. D* **43**, 104 (1991).
- [75] E. Eichten, I. Hinchliffe, K. Lane, and C. Quigg, *Rev. Mod. Phys.* **56**, 579 (1984) [*Addendum-ibid.* **58**, 1065 (1986)].
- [76] D. W. Duke and J. F. Owens, *Phys. Rev. D* **30**, 49 (1984).
- [77] D. Acosta *et al.* (CDF Collaboration), *Phys. Rev. D* **65**, 072005 (2002).
- [78] M. J. Tannenbaum, talk given at the Workshop on RHIC Paradigms, April 14–17, 2010, Austin, Texas, [arXiv:1008.1536](#) [nucl-ex].
- [79] B. Hippolyte, *Eur. Phys. J. C* **49**, 121 (2007).
- [80] B. Hippolyte, *Eur. Phys. J. C* **62**, 237 (2009).
- [81] H. Ricaud, A. Kalweit, and A. Maire, *J. Phys. G* **37**, 094049 (2010).
- [82] R. J. Fries, B. Muller, C. Nonaka, and S. A. Bass, *Phys. Rev. C* **68**, 044902 (2003).
- [83] V. Greco, C. M. Ko, and P. Levai, *Phys. Rev. C* **68**, 034904 (2003).
- [84] R. C. Hwa and C. B. Yang, *Phys. Rev. C* **67**, 034902 (2003).
- [85] B. I. Abelev *et al.* (STAR Collaboration), *Phys. Rev. C* **75**, 064901 (2007).
- [86] D. E. Acosta *et al.* (CDF Collaboration), *Phys. Rev. D* **72**, 052001 (2005).
- [87] CMS Collaboration, CERN CMS Physics Analysis Summary QCD-10-007 (2010) [<http://cdsweb.cern.ch/record/1279344>]; Keith A. Ulmer (CMS Collaboration), [arXiv:1012.1605](#) [hep-ex].
- [88] T. Sjostrand, S. Mrenna, and P. Z. Skands, *Comput. Phys. Commun.* **178**, 852 (2008).
- [89] T. Sjostrand, S. Mrenna, and P. Z. Skands, *J. High Energy Phys.* **05** (2006) 026.
- [90] K. Werner, T. Hirano, I. Karpenko, T. Pierog, S. Porteboeuf, M. Bleicher, and S. Haussler, *Nucl. Phys. Proc. Suppl.* **196**, 36 (2009).
- [91] K. Werner, I. Karpenko, and T. Pierog, *J. Phys. Conf. Ser.* **230**, 012026 (2010).
- [92] T. Alexopoulos *et al.* (E735 Collaboration), *Phys. Rev. D* **48**, 984 (1993).
- [93] M. Banner *et al.* (UA2 Collaboration), *Phys. Lett. B* **122**, 322 (1983).
- [94] P. Antonioli (ALICE Collaboration), to appear in the Proceedings of Hadron Collider Symposium (HCP2010), August 23–27, 2010, Toronto, Canada.

- [95] V. V. Skokov and P. Levai, *Phys. Rev. D* **78**, 054004 (2008).  
[96] P. Levai and V. Skokov, PoS **EPS-HEP2009**, 456 (2009).  
[97] A. Giovannini and R. Ugoccioni, *Eur. Phys. J. C* **36**, 309 (2004).  
[98] D. Kharzeev, *Phys. Lett. B* **378**, 238 (1996).  
[99] A. K. Aamodt *et al.* (ALICE Collaboration), *Phys. Rev. Lett.* **105**, 072002 (2010).  
[100] B. Z. Kopeliovich and B. Povh, *Phys. Lett. B* **446**, 321 (1999).